USCAP

www.nature.com/labinvest

ARTICLE

Check for updates

circHECTD1 attenuates apoptosis of alveolar epithelial cells in acute lung injury

Hongbin Li[1]✉, Xiaoxuan Niu[1], Huijuan Shi[1], Min Feng[1], Yuming Du[1], Rongqing Sun[1], Ning Ma[1], Haili Wang[1], Dan Wei[1] and Min Gao[1]✉

Circular RNAs (circRNAs) play important roles in many lung diseases. This study aimed to investigate the role of *circHECTD1* in acute lung injury (ALI). The mouse and cell models of ALI were induced by lipopolysaccharide (LPS). The apoptosis of alveolar epithelial cells (AECs) was detected by flow cytometry. The relationships between *circHECTD1*, miRNAs, and target genes were assessed by RNA pull-down, luciferase reporter gene, and RNA-FISH assays. *circHECTD1* was downregulated in LPS-induced human and mouse AECs (HBE and MLE-12). The knockdown of *circHECTD1* increased the apoptotic rates and the expressions of *miR-136* and *miR-320a*, while its overexpression caused opposite effects in LPS-induced HBE and MLE-12 cells. Mechanistically, *circHECTD1* bound to *miR-320a* and *miR-136*. *miR-320a* targeted PIK3CA and mediated the effect of *circHECTD1* on PIK3CA expression. *miR-136* targeted Sirt1 and mediated the effect of *circHECTD1* on Sirt1 expression. Silencing PIK3CA and/or Sirt1 reversed the effect of *circHECTD1* overexpression on the apoptosis of LPS-induced HBE and MLE-12 cells. In vivo, overexpression of *circHECTD1* alleviated the LPS-induced ALI of mice. Our findings suggested that *circHECTD1* inhibits the apoptosis of AECs through *miR-320a*/PIK3CA and *miR-136*/Sirt1 pathways in LPS-induced ALI.

Laboratory Investigation (2022) 102:945–956; https://doi.org/10.1038/s41374-022-00781-z

INTRODUCTION

Acute lung injury (ALI) is a common critical disease caused by various injury factors and characterized by respiratory distress, non-cardiogenic pulmonary edema, and persistent excessive inflammatory response[1,2]. As ALI progresses, it may even develop into acute respiratory distress syndrome (ARDS) and seriously threatens the health and life of the patient[3]. Although the pathogenesis of ALI has not been fully elucidated, the excessive apoptosis of alveolar epithelial cells (AECs) has been considered as a key pathological basis of ALI[4]. Under pathological conditions, AEC apoptosis can induce the damage of the alveolar epithelial barrier, which leads to alveolar cavity effusion and severe lung ventilation damage, thereby promoting the development of ALI[5,6]. Thus, exploring the molecular mechanism underlying ACE apoptosis is important for understanding the pathogenesis of ALI and its treatment.

Circular RNAs (circRNAs) are a class of novel non-coding RNAs that are widely expressed in mammalian cells and have tissue and developmental stage specificity[7]. It has been proven that the aberrant expression of circRNAs is closely related to many diseases, such as cancers and cardiovascular diseases[8–11]. Recent studies reported that many circRNAs are dysregulated in smoke inhalation-induced ALI rats and lipopolysaccharide (LPS)-induced ALI mice[12,13], implying that circRNAs may play important roles in ALI. Circular RNA HECT domain E3 ubiquitin-protein ligase 1 (*circRNA HECTD1*) derives from the exon 23 and 24 of the *HECTD1* gene and has been confirmed to be involved in many diseases, including gastric cancer, acute ischemic stroke, and silicosis[14–17]. Besides, Ye et al., found that *circRNA HECTD1* was downregulated in the bronchoalveolar lavage fluid and lung tissues of ALI rats[12]. However, the role and the underlying mechanism of *circHECTD1* in ALI remain unclear.

Mechanistically, circRNAs usually exert their functions in many diseases by acting as microRNA (miRNA) sponges to regulate the expressions of miRNA target genes[18]. For instance, circBPTF contributes to the progression and recurrence of bladder cancer through the *miR-31-5p*/RAB27 pathway[19]. *circPTPRA* represses the epithelial-mesenchymal transitioning and metastasis of non-small-cell lung cancer cells by sponging *miR-96-5p*[20]. Recent studies also indicate that *circHECTD1* can promote gastric cancer progression via sponging *miR-1256* and upregulating USP5 expression[15]. Moreover, *circHECTD1* can bind to *miR-142* to increase TIPARP expression, thereby promoting astrocyte autophagy in cerebral ischemic stroke[21]. Our bioinformatics analysis showed that there are predicted binding sites of *miR-136* and *miR-320a* on *circHECTD1*. Our further preliminary experiments revealed that *circHECTD1* expression was decreased in LPS-treated human and mouse AECs, and its knockdown upregulated the expressions of *miR-136* and *miR-320a* in AECs. However, whether *circHECTD1* can regulate AEC apoptosis in ALI by acting as sponges of *miR-136* and *miR-320a* is still unknown.

In this study, we aimed to investigate the role and mechanism of *circHECTD1* in ALI. Here, we found that the overexpression of *circHECTD1* inhibited LPS-induced apoptosis of human and mouse

[1]Department of Critical Care Medicine, the First Affiliated Hospital of Zhengzhou University, Zhengzhou 450052 Henan Province, China. ✉email: lihongbin2006@126.com; gaomin0033@126.com

Received: 7 July 2021 Revised: 21 February 2022 Accepted: 4 March 2022
Published online: 19 April 2022

AECs. Mechanistically, we confirmed that *circHECTD1* inhibited LPS-induced AEC apoptosis by regulating *miR-320a*/PIK3CA and *miR-136*/Sirt1 pathways, thereby relieving the LPS-induced ALI of mice. These findings demonstrated a novel role of circRNAs in regulating AECs during ALI and implied that *circHECTD1* may be a therapeutic target of ALI.

MATERIALS AND METHODS

Animal and ALI model establishment

C57BL/6 mice (5–6 weeks of age; 18–20 g) were purchased from the Experimental Animal Center of Henan Province and were housed under the standard conditions of temperature, light, and humidity control. All mice had easy access to food and water. The animal experiments were performed in the Laboratory Animal Center of Zhengzhou University and approved by the Animal Ethics Committee of the First Affiliated Hospital of Zhengzhou University.

The mouse model of ALI was induced by LPS administration[22]. In brief, mice were treated with 1 mg/kg of LPS via intra-tracheal instillation. Mice in the control group were intratracheally instilled with 1 mg/kg of saline. During 0–48 h, mouse survival was monitored; 48 h after LPS treatment, mice were sacrificed by intraperitoneal injection of an overdose of pentobarbital. Lung tissues were isolated and collected for further study.

Adenovirus vectors injection

Ad carrying green fluorescent protein (GFP) and *circHECTD1* (Ad-*circHECTD1*) was obtained from FitGene Biotechnology Co. (Guangzhou, China). Ad only containing GFP was utilized as the negative control (Ad-GFP). ALI mice were divided into two groups: the Ad-*circHECTD1* group ($n = 7$) and the Ad-GFP group ($n = 7$). Seven days before LPS administration, mice in the Ad-*circHECTD1* group were anesthetized using sodium pentobarbital, and then intratracheally instilled with 1×10^9 U Ad-*circHECTD1* as previously described[22]. Mice in the Ad-GFP group were intratracheally instilled with 1×10^9 U Ad-GFP.

Histological staining of the lung

The mouse lung tissues were fixed with 4% paraformaldehyde before being washed with distilled water. Then lung tissues were dehydrated with gradient ethanol, rendered transparent with xylene, and embedded in paraffin. Next, lung tissues were sliced into 5 μm sections. For HE staining, cells were stained by hematoxylin and eosin using the Hematoxylin and Eosin Staining Kit (Beyotime, China). For TUNEL staining, the Colorimetric TUNEL Apoptosis Assay Kit (Beyotime) was utilized. The stained sections were observed under a microscope (Olympus, Japan).

At least four slides per lung were selected to determine the number of cells exhibiting TUNEL-positive staining for apoptosis. For each slide, 5 fields were randomly chosen, and a total of TUNEL-positive cells per field were counted using a defined rectangular field area. The number of apoptosis was determined from a total of 20 fields per lung tissues (TUNEL-positive cells/field).

Cell culture and treatment

Human bronchial epithelial cells (HBE) and mouse AECs (MLE-12) were purchased from ATCC (VA, USA). HBE and MLE-12 cells were cultured in RPMI 1640 medium supplemented with 10% fetal bovine serum and incubated in 5% CO_2 at 37 °C. Cells were treated with 100 mg/ml LPS for 24 h to induce the ALI model in vitro.

Cell transfection

The Ad vectors expressing PIK3CA (Ad-PIK3CA) or Sirt1 (Ad-Sirt1) were obtained from the FitGene Biotechnology Co. (Guangzhou, China). The overexpression vectors (*miR-320a* mimic and *miR-136* mimic) and the silence vectors (*miR-320a* inhibitor, *miR-136* inhibitor, si-*circHECTD1*-1, si-*circHECTD1*-2, si-Sirt1, and si-PIK3CA) were obtained from GeneChem Co. Ltd. (Shanghai, China). Cell transfections were performed using Lipofectamine 2000 (Invitrogen, USA). The sequences of siRNA and RNA oligonucleotides have provided in Supplemental Material.

RNA-FISH

Fluorescent probes targeting *circHECTD1* (cy3-labeled), *miR-320a* (cy5-labeled), and *miR-136* (cy5-labeled) were designed for circHECTD1 in situ hybridization. The 4,6-diamidino-2-phenylindole (DAPI) was used to stain nuclei. Hybridization was performed using Fluorescent in Situ Hybridization Kit (RiboBio, China) according to the manufacturer's instructions. Cells were analyzed by Nikon A1Si Laser Scanning Confocal Microscope (Nikon, Japan). The quantification of co-localization was performed as described previously[23]. The sequences of Fish probe have provided in Supplemental Material.

Bioinformatics analysis

Bioinformatics databases Circular RNA Interactome (https://circinteractome.nia.nih.gov/) and ENCORI for RNA Interactomes (https://starbase.sysu.edu.cn/) were used for detecting the binding site between miRNAs (*miR-136*, *miR-142*, *miR-335*, *miR-199*, *miR-515*, *miR-519*, *miR-561*, and *miR-320a*) and *circHECTD1*. Bioinformatics databases ENCORI for RNA Interactomes, miRanda, targetScan (http://www.targetscan.org/vert_80/), and RNAInter (http://www.rnainter.org) were used for predicting the binding sites of miR-320a on PIK3CA 3′ UTR, miR-136 on the 3′-UTR of Sirt1.

Luciferase reporter assay

circHECTD1 was cloned into plasmid expressing luciferase and named LUC-circHECTD1. Then, LUC-*circHECTD1* was co-transfected into 293 T cells with *miR-136* mimic and/or *miR-320a* mimic. The luciferase activity of LUC-circHECTD1 was detected 48 h after transfection, using the Dual-Luciferase Reporter System Kit (Promega, USA). The pre-NC was used as a negative control of miRNA mimics.

The wild type (WT) 3′-UTR sequences of PIK3CA (PIK3CA-WT) and Sirt1 (Sirt1-WT) and the mutated (MUT) 3′-UTR sequences of PIK3CA (PIK3CA-MUT) and Sirt1 (Sirt1-MUT) were cloned into plasmids expressing luciferase and named LUC-PIK3CA-WT, LUC-Sirt1-WT, LUC-PIK3CA-MUT, and LUC-Sirt1-MUT. Each of these recombinant vectors was co-transfected into 293 T cells with *miR-136* mimic or *miR-320a* mimic or pre-NC.

Flow cytometry

The apoptosis of HBE and MEL-12 cells was detected using Annexin V-FITC Apoptosis Detection Kit (Beyotime, China). Briefly, 5×10^4 HBE or MEL-12 cells were centrifuged at 1000 g for 5 min and the supernatant was removed. Then cells were resuspended in 195 μl Annexin V-FITC binding buffer. Later, cells were incubated with 5 μl Annexin V-FITC and 10 μl PI at room temperature for 15 min and then were acquired through a flow cytometer (BD Biosciences, USA). The FlowJo software was used for the analysis of apoptotic cells.

RNA pull-down assay

HBE cells (1.5×10^7) were collected and lysed by lysis buffer. The biotin-labeled *circHECTD1* probe was obtained from Genepharm (Shanghai, China). After incubation with streptavidin agarose beads, the *circHECTD1* probe was incubated with a lysate of HBE cells at 4 °C for the whole night. Then the pulled-down complex of the *circHECTD1* probe was used for RNA purification. The enrichment of *miR-136* and *miR-320a* in the complex was detected by qPCR. The oligonucleotide (oligo) probe was used as a negative control of the *circHECTD1* probe. The sequences of *circHECTD1* probe have provided in Supplemental Material.

Real-time fluorescent quantitative PCR

Total RNA was extracted from mouse lung tissues and cells (HBE and MLE12) using Trizol reagent (Invitrogen, USA). After qualitative and quantitative analysis, 1 μg RNA reversed to cDNA using PrimeScript II 1st Strand cDNA Synthesis Kit (Takara, Japan). Then the cDNA was utilized to perform real-time fluorescent quantitative PCR (qRT-PCR) using One-Step TB Green PrimeScript PLUS RT-PCR Kit (Takara). The relative expressions of genes were calculated by the $2^{-\Delta\Delta CT}$ method. GAPDH was employed as an internal reference for circRNAs, PIK3CA, and Sirt1. U6 was used as an internal reference for miRNAs. The sequences of primers have provided in Supplemental Figs. 1–4.

Western blot

Mouse lung tissues and cells (HBE and MLE12) were lysed by RIPA lysis buffer containing protease inhibitors and then were centrifuged to obtain protein. The concentration of protein samples was determined by Micro BCA™ Protein Assay Kit (Thermo Scientific, USA). Then 30 μg protein of each sample was taken for SDS-PAGE. After separation by SDS-PAGE, proteins were transferred onto polyvinylidene fluoride (PVDF) membranes

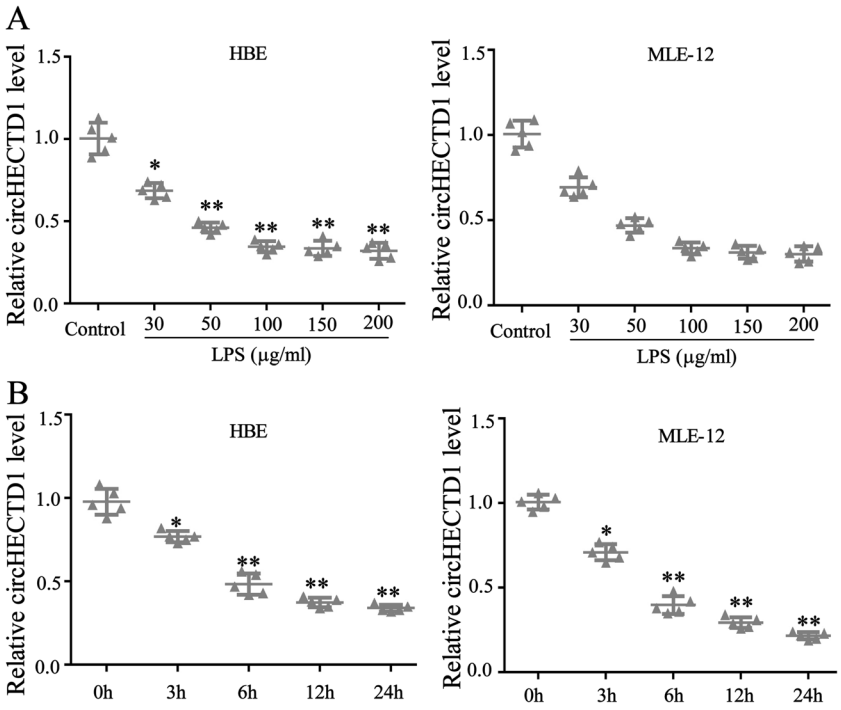

Fig. 1 The expression of *circHECTD1* in LPS-induced alveolar epithelial cells (AECs). A HBE and MLE-12 cells were treated with LPS (0, 30, 50, 100, 150, 200 μg/ml) for 6 h. The expression of *circHECTD1* in cells was detected by qRT-PCR. **B** HBE and MLE-12 cells were treated with 100 μg/ml LPS for 0, 3, 6, 12, and 24 h. The expression of *circHECTD1* in cells was detected by qRT-PCR. *$p < 0.05$,**$p < 0.01$ vs. control or 0 h.

and then blocked for 1 h. Next, the PVDF membranes were incubated with primary antibodies: anti-PIK3CA (1:1000, ab40776, Abcam), anti-Sirt1 (1:2000, ab189494, Abcam), anti-Akt (1:500, ab38449, Abcam), anti-p-Akt (1:1000, ab38449, Abcam), anti-Bad (1:1000, ab32445, Abcam), anti-Bax (1:2000, ab32503, Abcam), anti-Caspase-9 (1:2000, ab32539, Abcam), anti-cleaved-Parp (1:1000, ab32064, Abcam), anti-cleaved-caspase-3 (1:500, ab32042, Abcam), anti-Bcl-2 (1:1000, ab32124, Abcam) and anti-GAPDH (1:3000, ab8245, Abcam) at 4°C overnight, followed by incubation with corresponding secondary antibody (1:5000, ab6721, Abcam) at room temperature for 2 h. The protein blots were visualized using enhanced chemiluminescence (Thermo Scientific). GAPDH was used as an internal reference.

Statistical analysis

All data were analyzed using GraphPad Prism 7.0 software and expressed as the mean ± standard error of the mean (SEM). Two-tailed paired Student's t-test (for 2 groups) or One-way ANOVA (for more than 2 groups) were used to calculate statistical differences in mean values between groups. Statistical significance was set as *$p < 0.05$ and **$p < 0.01$. For the in vitro study, all experiments were repeated three times.

RESULTS

circHECTD1 was down-regulated in LPS-induced AECs

As shown in Fig. 1A and Fig. S1, we detected the expressions of 10 circRNAs (*circHECTD1*, *circCDYl2*, *circTTC3*, *circHIPK3*, *circPTEN*, *circITGAM*, *circADGRF5*, *circFKBP5*, *circBACH1*, and *circPRKD1*) in LPS-induced AECs that were reported to be dysregulated in ALI[12,13]. We found that only the expression trend of *circHECTD1* was consistent in LPS-induced human and mouse alveolar epithelial cells (HBE and MLE-12). Moreover, *circHECTD1* expression showed a decrease to the greatest extent in 100 μg/ml LPS-induced HBE and MLE-12 cells (Fig. 1A). When the concentration of LPS was higher than 100 μg/ml, *circHECTD1* expression did not continue to decline (Fig. 1A). Therefore, we chose 100 μg/ml LPS to induce cells in the following experiment. We then detected the expression of *circHECTD1* in HBE and MLE-12 cells during LPS treatment at different times. The results showed that LPS reduced the expression of *circHECTD1* in HBE and MLE-12 cells in a time-dependent manner (Fig. 1B). Thus, *circHECTD1* was selected for further experiments in this study.

circHECTD1 regulated the apoptosis of AECs

The effects of *circHECTD1* knockdown and overexpression on the apoptosis of AECs were assessed. As shown in Fig. 2A, si-*circHECTD1*-1 and si-*circHECTD1*-2 effectively decreased *circHECTD1* expression in HBE and MLE-12 cells. In response to *circHECTD1* knockdown, cell apoptosis was increased in HBE and MLE-12 cells (Fig. 2B, C). As shown in Fig. 2D–F, the overexpression of *circHECTD1* significantly decreased the LPS-induced cell apoptosis in HBE and MLE-12 cells.

circHECTD1 bound to miR-136 and miR-320a in the AECs

Based on the bioinformatics databases Circular RNA Interactome and ENCORI for RNA Interactomes, we found 8 miRNAs (*miR-136*, *miR-142*, *miR-335*, *miR-199*, *miR-515*, *miR-519*, *miR-561*, and *miR-320a*) that have potential binding sites with *circHECTD1* (Fig. S2). To determine the specific target miRNAs of *circHECTD1* in AECs, the expression levels of 8 candidate miRNAs were detected in HBE cells transfected with si-*circHECTD1*-1, si-*circHECTD1*-2 or si-control. As shown in Fig. 3A, the knockdown of *circHECTD1* significantly increased the expressions of *miR-136* and *miR-320a* in HBE cells, while having no evident effect on the expressions of the other 6 miRNAs. Then the effects of *circHECTD1* on the expressions of *miR-136* and *miR-320a* were determined in HBE cells. The results revealed that LPS treatment increased the expressions of *miR-136* and *miR-320a*, while *circHECTD1* overexpression abolished this upregulation (Fig. 3B). To verify whether *circHECTD1* can bind to *miR-136* and *miR-320a* in the pulmonary epithelium, the luciferase reporter gene assay, FISH assay, and RNA pull-down assay were performed. The result of luciferase reporter gene assay showed that overexpression of *miR-136* or

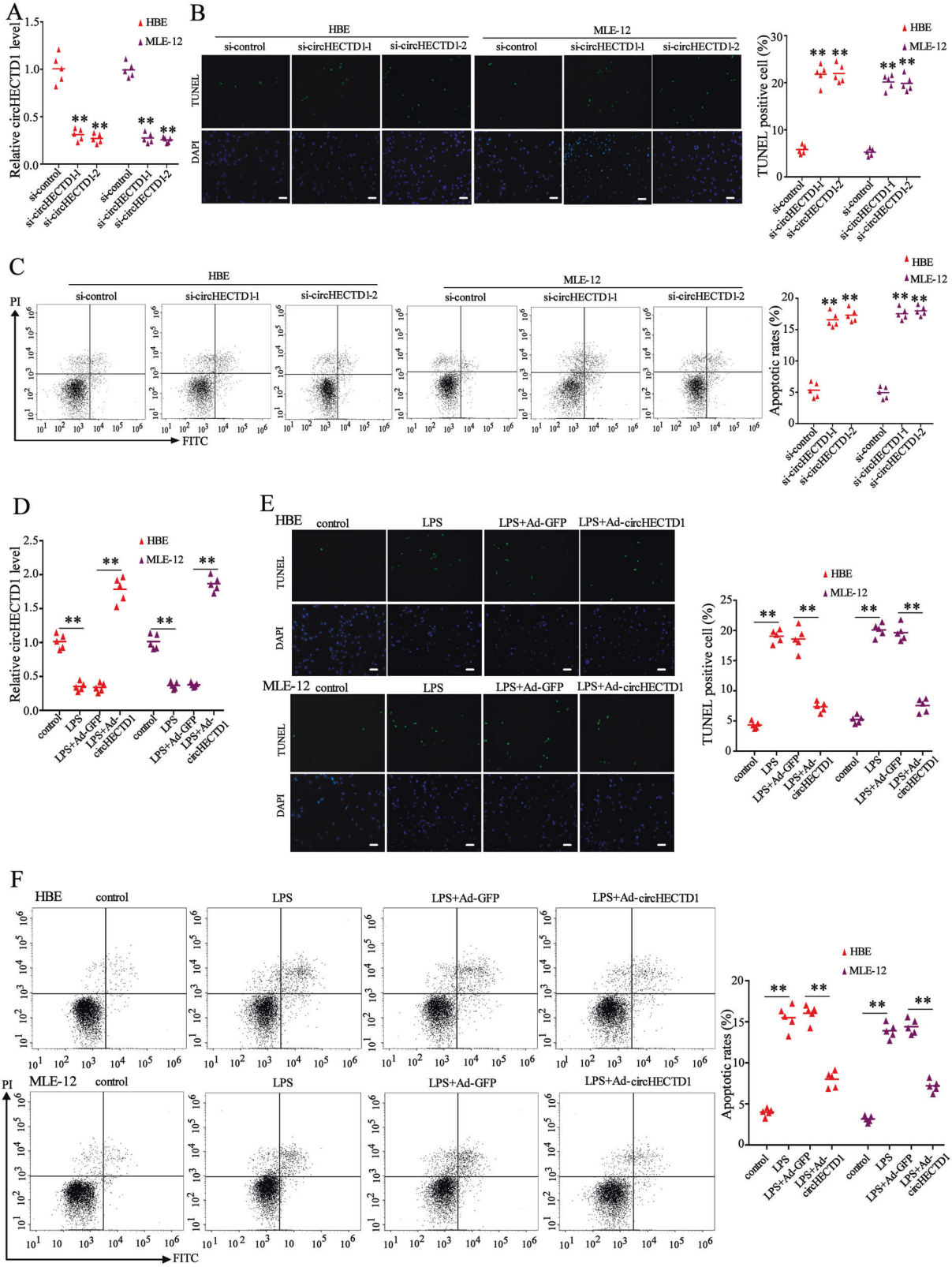

Fig. 2 The effect of *circHECTD1* on the apoptosis of AECs. A–C HBE and MLE-12 cells were transfected with si-*circHECTD1*-1, si-*circHECTD1*-2 or its negative control (si-control). **A** The *circHECTD1* expression was measured by qRT-PCR. **B** The representative images of TUNEL staining (Scale bar = 50 μm). **C** The cell apoptosis was detected by flow cytometry (**$p < 0.01$ vs. si-control). **D–F** HBE and MLE-12 cells were transfected with Ad-*circHECTD1* or its negative control (Ad-GFP) and then treated with 100 μg/ml LPS. **D** The *circHECTD1* expression was measured by qRT-PCR. **E** The representative images of TUNEL staining (Scale bar = 50 μm). **F** The apoptosis of HBE and MLE-12 cells was detected by flow cytometry. **$p < 0.01$.

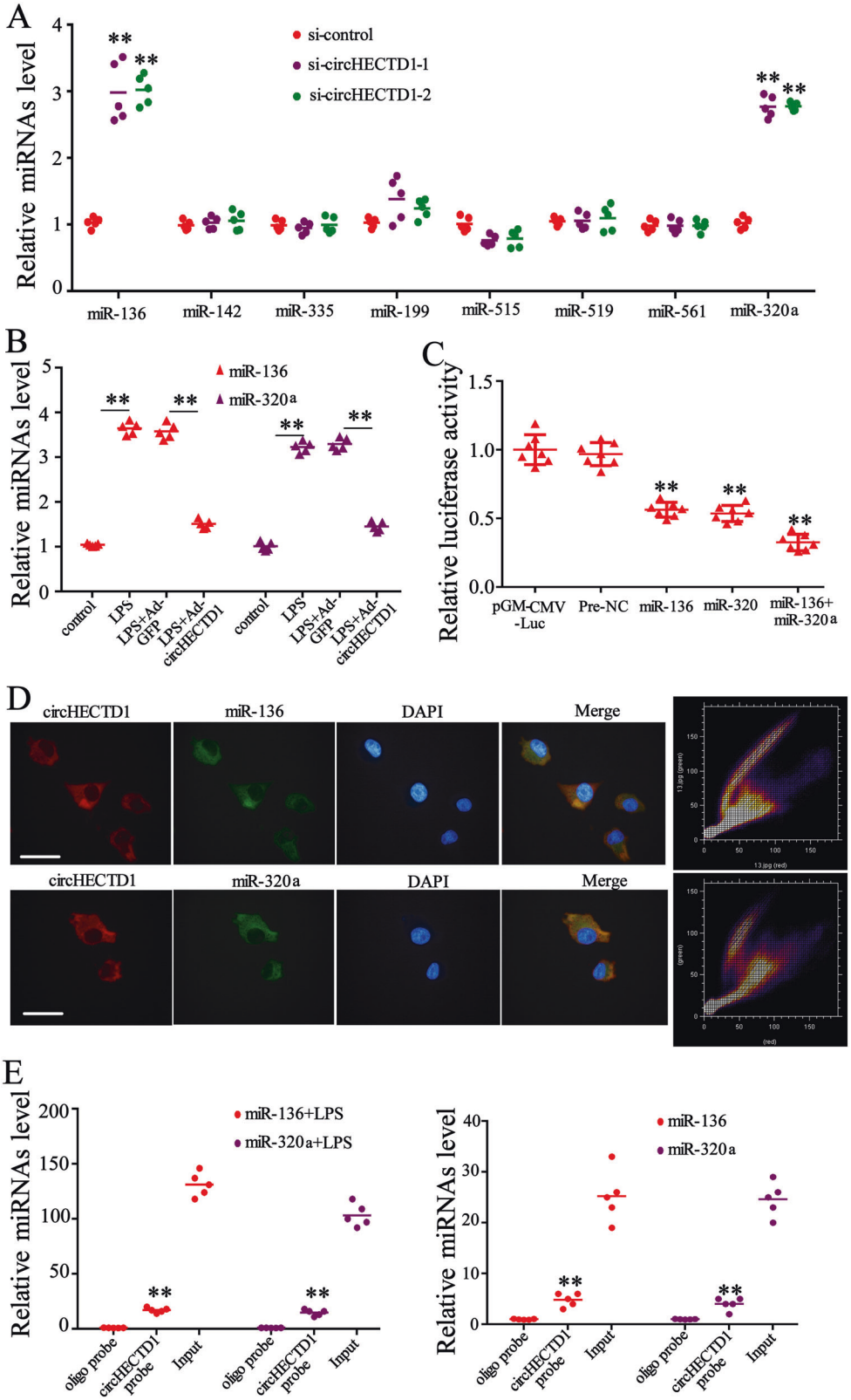

Fig. 3 ***circHECTD1* binds to *miR-136* and *miR-320* in AECs. A** HBE cells were transfected with si-control or si-*circHECTD1*-1, si-*circHECTD1*-2. The expressions of miRNAs were detected by qRT-PCR (**$p < 0.01$ vs. si-control). **B** HBE cells were transfected with Ad-circHECTD1 or Ad-GFP and then treated with 100 μg/ml LPS for 6 h. The expressions of *miR-136* and *miR-320a* were detected by qRT-PCR (**$p < 0.01$). **C** 293 T cells were co-transfected with the LUC-*circHECTD1* vector and *miR-136* mimic (and/or *miR-320a* mimic). Then the luciferase activity of LUC-*circHECTD1* was detected (**$p < 0.01$ vs. pre-NC). pre-NC: negative control of *miR-136* and *miR-320a* mimic. pGM-CMV-Luc: positive control. **D** The colocalization of *circHECTD1* with *miR-136* or *miR-320a* by FISH assay. Bar = 10 μm. The two panels on the right represented red and green pixel intensities of circHECTD1 and miR-136/miR-320a FISH image. **E** qRT-PCR was used to determine the enrichment of *miR-136* and *miR-320a* in the *circHECTD1* probe pulled-down complex in HBE cells treated with or without LPS. **$p < 0.01$ vs oligo probe.

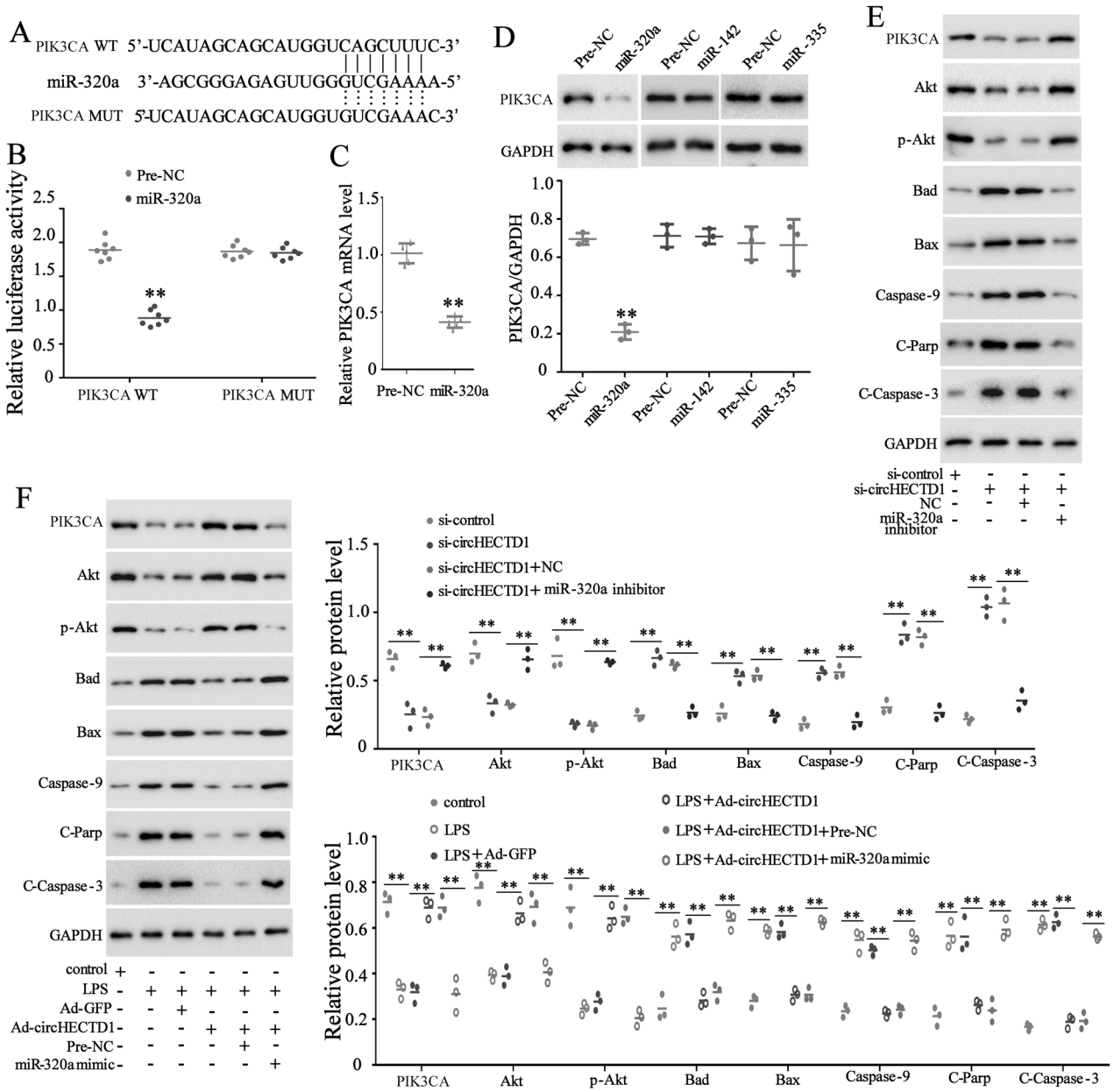

Fig. 4 ***circHECTD1*** **regulates PIK3CA expression through** ***miR-320a*****. A** The binding site of *miR-320a* on *PIK3CA* mRNA 3′ UTR. **B** 293 T cells were co-transfected with *miR-320a* (or pre-NC) and LUC-PIK3CA-WT (or LUC-PIK3CA-MUT). Then the luciferase activities of LUC-PIK3CA-WT and LUC-PIK3CA-MUT were detected (**$p < 0.01$ vs pre-NC + LUC-PIK3CA-WT). **C** HBE cells were transfected with *miR-320a* mimic or pre-NC. The mRNA level of *PIK3CA* was detected by qRT-PCR. **D** HBE cells were transfected with *miR-320a* mimic, *miR-142* mimic, *miR-335* mimic, or pre-NC. The protein level of PIK3CA was detected by western blot. **E** HBE cells were transfected with si-*circHECTD1* and/or *miR-320a* inhibitor or corresponding controls. The protein levels of PIK3CA, Akt, p-Akt, Bad, Bax, and Caspase-9 were detected by western blot. **F** HBE cells were transfected with Ad-*circHECTD1* and/or *miR-320a* mimic or corresponding controls and then treated with 100 μg/ml LPS. The protein levels of PIK3CA, Akt, p-Akt, Bad, Bax, Caspase-9, cleaved-Parp (C-Parp) and cleaved-caspase-3 were detected by western blot. NC: negative control of *miR-320a* inhibitor; pre-NC: negative control of *miR-320a* mimic. **$p < 0.01$ vs pre-NC.

miR-320a significantly reduced the luciferase activity of LUC-*circHECTD1*, and the simultaneous overexpression of *miR-136* and *miR-320a* decreased the luciferase activity of LUC-*circHECTD1* to a greater extent (Fig. 3C). The FISH assay showed that *circHECTD1* was co-located with *miR-136* and *miR-320a* in the cytoplasm of HBE cells (Fig. 3D). The RNA pull-down assay revealed that *miR-136* and *miR-320a* were enriched in the complexes pulled down by the *circHECTD1* probe in HBE cells treated with or without LPS (Fig. 3E). These results showed that *circHECTD1* can bind to *miR-136* and *miR-320a* in the AECs.

miR-320a mediated the regulatory effect of circHECTD1 on PIK3CA expression

Given that the bioinformatics databases (ENCORI for RNA Interactomes, miRanda, targetScan, and RNAInter) predicted that there were binding sits of *miR-320a* on PIK3CA 3′ UTR (Fig. 4A), we then confirmed whether *miR-320a* can target PIK3CA. The result of luciferase reporter gene assay showed that *miR-320a* overexpression significantly reduced the luciferase activity of LUC-PIK3CA-WT, while having no significant effect on the luciferase activity of LUC-PIK3CA-MUT (Fig. 4B). The qRT-PCR analysis revealed that

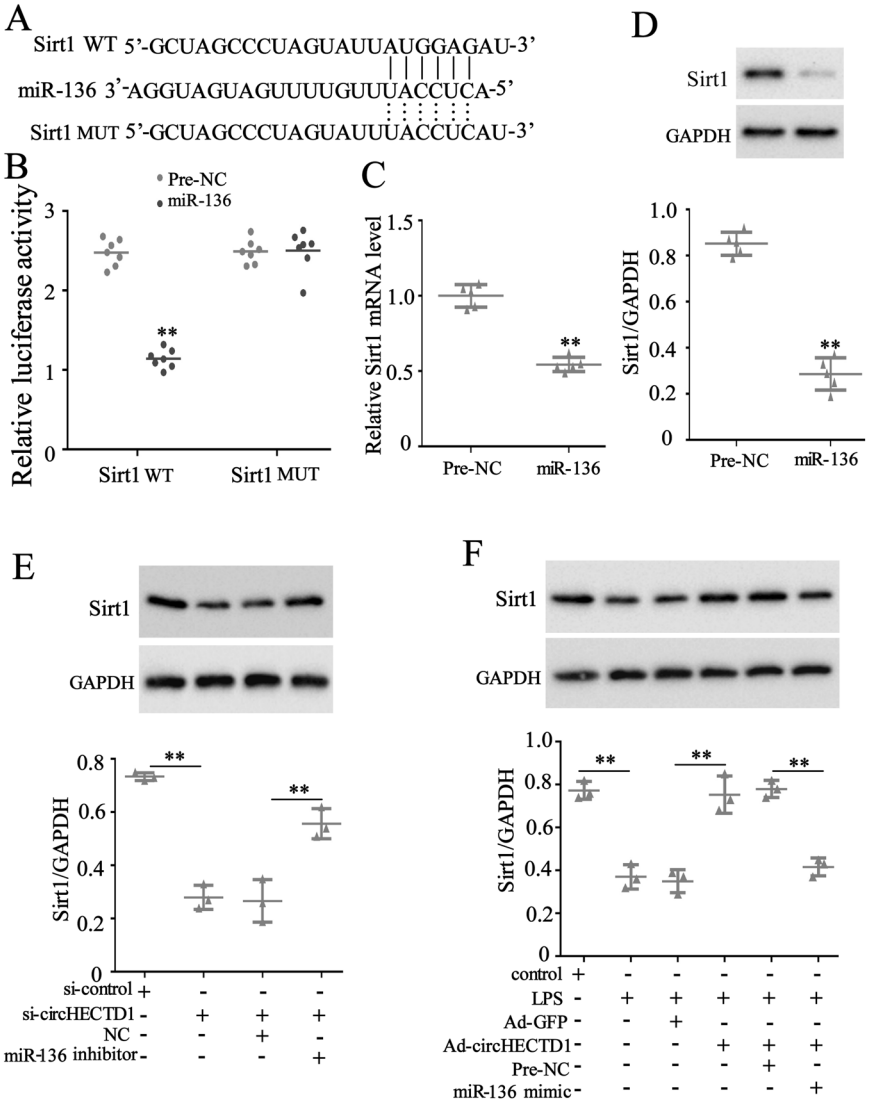

Fig. 5 ***circHECTD1*** **regulates Sirt1 expression through** ***miR-136*****.** **A** The binding site of *miR-136* on Sirt1 3′-UTR. **B** 293 T cells were co-transfected with *miR-136* (or pre-NC) and LUC-Sirt1-WT (or LUC-Sirt1-MUT). Then the luciferase activities of LUC-Sirt1-WT and LUC-Sirt1-MUT were detected (**$p < 0.01$ vs pre-NC + LUC-Sirt1-WT). **C**, **D** HBE cells were transfected with *miR-136* mimic or pre-NC. The expression of Sirt1 was detected by qRT-PCR and western blot. **E** HBE cells were transfected with si-*circHECTD1* and/or *miR-136* inhibitor or corresponding controls. The protein level of Sirt1 was detected by western blot. **F** HBE cells were transfected with Ad-*circHECTD1* and/or *miR-136* mimic or corresponding controls and then treated with 100 μg/ml LPS. The protein level of Sirt1 was detected by western blot. NC: negative control of *miR-136* inhibitor; pre-NC: negative control of *miR-136* mimic. **$p < 0.01$ vs pre-NC.

miR-320a overexpression decreased the mRNA level of *PIK3CA* in HBE cells (Fig. 4C). In addition, the PIK3CA protein was lessened by *miR-320a* mimic transfection but not *miR-142* mimic /*miR-335* mimic /pre-NC transfection, which further confirmed that PIK3CA was specifically regulated by *miR-320a* (Fig. 5C). Then we verified whether *miR-320a* mediates the effect of *circHECTD1* on the PIK3CA pathway. We observed that the *circHECTD1* silence reduced the protein levels of PIK3CA, AKT, and p-AKT and elevated the protein levels of Bad, Bax, Caspase-9, cleaved-Parp (C-Parp) and cleaved-caspase-3 in HBE cells, whereas *miR-320a* knockdown reversed these effects (Fig. 4E). Furthermore, the overexpression of *circHECTD1* increased the protein levels of PIK3CA, AKT, and p-AKT and decreased the protein levels of Bad, Bax, Caspase-9, C-Parp and cleaved-caspase-3 in LPS-induced HBE cells, while *miR-320a* overexpression abrogated these impacts (Fig. 4F). These findings suggested that *miR-320a* mediated the regulation of *circHECTD1* on PIK3CA expression.

miR-136 mediated the regulation of circHECTD1 on Sirt1 expression

According to the bioinformatics databases (ENCORI for RNA Interactomes, miRanda, targetScan, and RNAInter), there was a binding site of *miR-136* on the 3′-UTR of Sirt1 (Fig. 5A), implying that *miR-136* might target Sirt1. As shown in Fig. 5B, the luciferase reporter gene assay revealed that the overexpression of *miR-136* decreased the luciferase activity of LUC-Sirt1-WT, while having no significant effect on the luciferase activity of LUC-Sirt1-MUT. The overexpression of *miR-136* also reduced the mRNA and protein levels of Sirt1 in HBE cells (Fig. 5C and D). We then investigated whether *miR-136* mediates the effect of *circHECTD1* on Sirt1 expression. We found that silencing *circHECTD1* inhibited the expression of Sirt1 in HBE cells, and this effect was reversed by *miR-136* knockdown (Fig. 5E). Moreover, the Sirt1 expression was elevated by *circHECTD* overexpression in LPS-induced HBE cells, whereas this trend was abolished by the forced expression of *miR-*

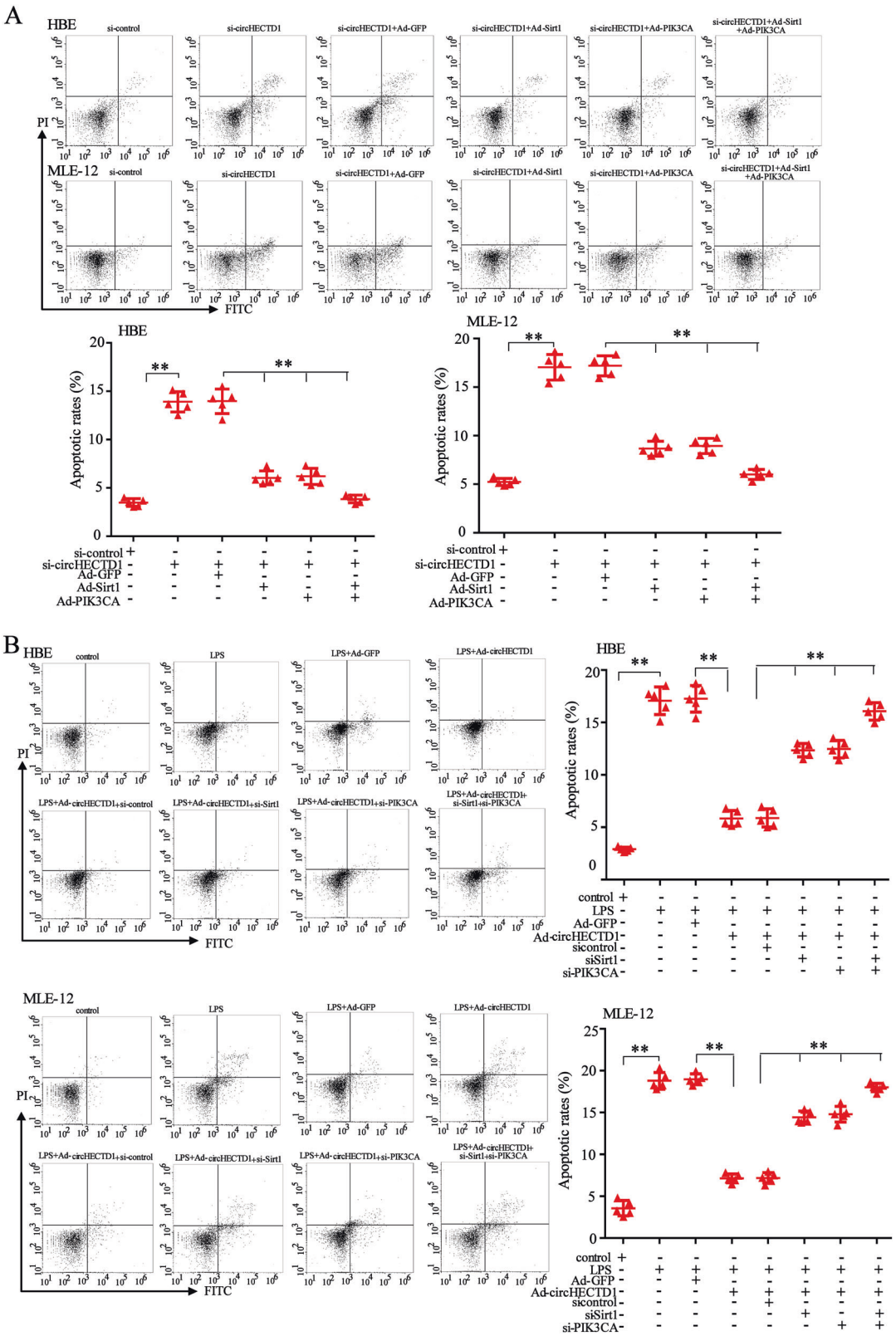

Fig. 6 Sirt1 and PIK3CA mediate the effect of *circHECTD1* on apoptosis of AECs. A HBE and MLE-12 cells were grouped as shown in the figure. The apoptosis of cells was detected by flow cytometry. **B** HBE and MLE-12 cells were transfected with indicated plasmids and then treated with 100 μg/ml LPS. The apoptosis of cells was detected by flow cytometry. $^{**}p < 0.01$.

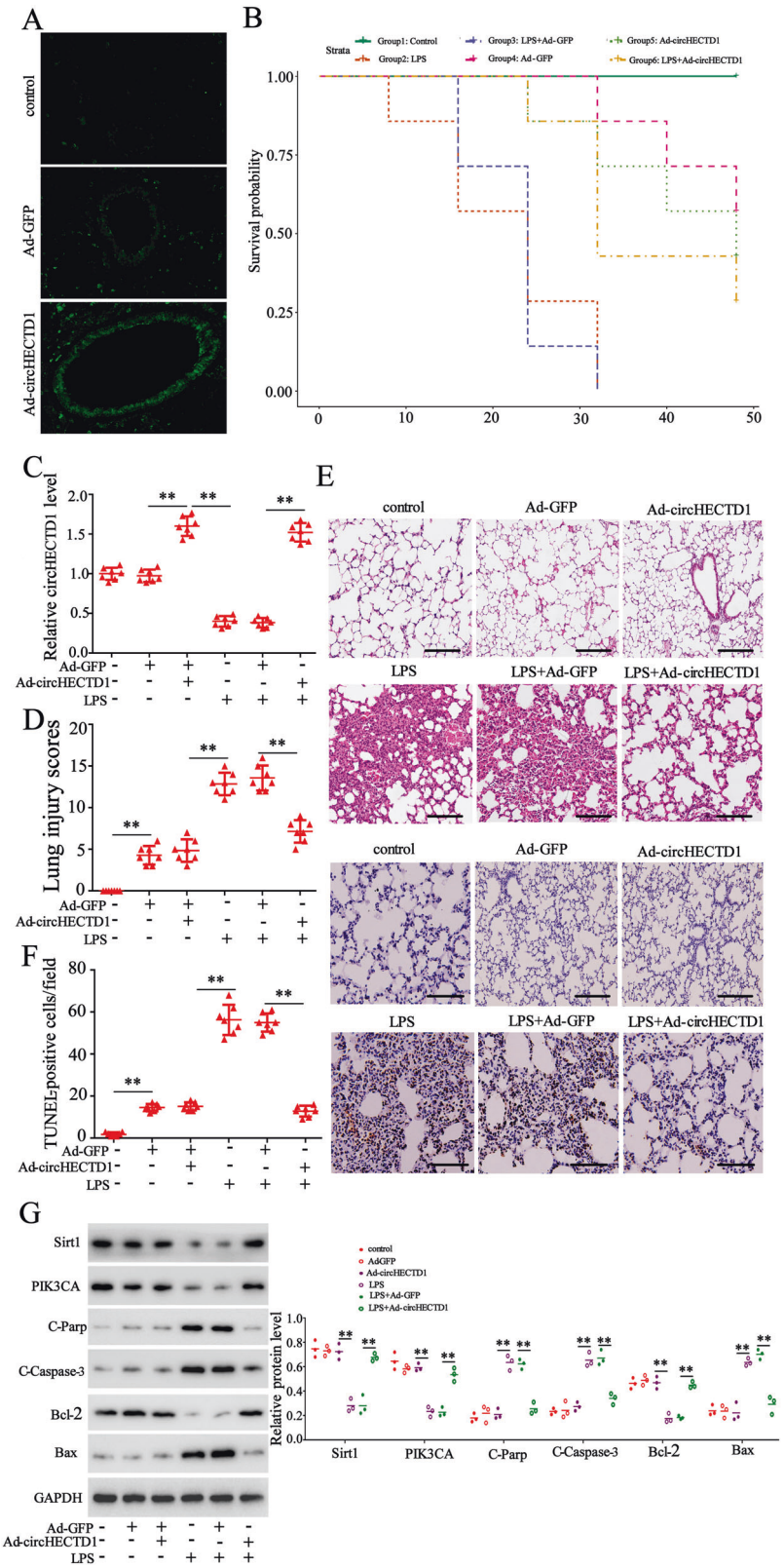

Fig. 7 ***circHECTD1* relieves ALI of mice. ALI mice were divided into two groups: the Ad-*circHECTD1* group ($n = 7$) and the Ad-GFP group ($n = 7$).** **A** Lung tissue section was obtained. Detection of the delivery of *circHECTD1* or GFP to the alveolar by fluorescence microscope. **B** The effect of *circHECTD1* overexpression on the survival rate of ALI mice. **C** The expression of *circHECTD1* was detected by qRT-PCR. **D** The effect of *circHECTD1* overexpression on lung injury scores. **E** The histopathological changes of lung tissues (Scale bar = 50 μm). **F** Representative images and quantitation of TUNEL staining performed on lung tissues (Scale bar = 50 μm). **G** The protein levels of Sirt1, PIK3CA, cleaved-Parp, cleaved-caspase-3, Bax and Bcl-2 were detected by western blot. $^{**}p < 0.01$.

136 (Fig. 5F). These findings suggested that *miR-136* mediated the regulation of *circHECTD1* on Sirt1 expression.

circHECTD1 regulated the apoptosis of AECs through Sirt1 and PIK3CA

Next, we explored whether *circHECTD1* regulated the apoptosis of AECs through Sirt1 and PIK3CA. We first detected *circHECTD1*, and the *Sirt1* and *PIK3CA* mRNA and protein expression levels under different transfection conditions, and the results showed that the AECs were successfully transfected (Fig. S3). As shown in Fig. 6A, the knockdown of *circHECTD1* increased the apoptotic rate of HBE and MLE-12 cells, while the overexpression of Sirt1 and/or PIK3CA reversed this impact. Meanwhile, the forced expression of *circHECTD1* decreased the apoptotic rate of LPS-induced HBE and MLE-12 cells, whereas the silence of Sirt1 and/or PIK3CA abolished this effect (Fig. 6B). These results implied that *circHECTD1* regulated the apoptosis of AECs through Sirt1 and PIK3CA.

circHECTD1 overexpression alleviated LPS-induced ALI of mice

To confirm the role of *circHECTD1* in ALI in vivo, we induced the mouse model of ALI by LPS treatment and injected adenovirus (Ad)-*circHECTD1* into ALI mice. As shown in Fig. 7A and C, Ad-*circHECTD1* was successfully delivered to the alveolar and upregulated the *circHECTD1* expression. As shown in Fig. 7B, LPS-induced ALI mice had a lower survival rate compared with control mice, while Ad-*circHECTD1* injection increased the survival rate of ALI mice. The results showed that the Ad-*circHECTD1* injection reduced the lung injury scores of LPS-induced ALI mice (Fig. 7D). The results of HE staining revealed that control mice had a clear and complete lung structure and a thin alveolar wall. The LPS-induced ALI mice showed evident lung injury, indicated by a disordered lung structure, a thick alveolar wall, and inflammatory cell infiltration. Compared with LPS-induced ALI mice, LPS + Ad-*circHECTD1* mice had a thinner alveolar wall and only slight inflammatory infiltration in lung tissues (Fig. 7E). Meanwhile, Ad-*circHECTD1* injection reduced LPS-induced cell apoptosis in ALI mice (Fig. 7F). Furthermore, the injection of Ad-*circHECTD1* increased the expression levels of Sirt1, PIK3CA and Bcl-2 in the lung tissues of ALI mice compare to LPS + Ad-GFP group (Fig. 7G). The *circHECTD1* overexpression reduced the protein levels of Bax, C-Parp and cleaved-caspase-3 (Fig. 7G). These results indicated that *circHECTD1* overexpression relieved LPS-induced ALI of mice.

DISCUSSION

Increasing numbers of studies have reported that dysregulated circRNAs play important roles in the pathological processes of multiple diseases, such as cancers[20,24], orthopedic[25,26], cardiovascular[9], and lung diseases[27]. *circHECTD1* is a novel circRNA and its aberrant expression is associated with many diseases. For example, Cai et al. reported that the expression of *circHECTD1* is increased in gastric cancer (GC) and its knockdown inhibits the progression of GC by blocking glutaminolysis[15]. Fang et al., pointed out that the upregulated *circHECTD1* facilitated the endothelial–mesenchymal transition of endothelial cells and macrophage activation in silicosis[14,28]. Recent studies show that many circRNAs are abnormally expressed in ALI, including *circHECTD1*[12]. Nevertheless, the role of *circHECTD1* in ALI has not been determined. Since the previous studies have indicated that AECs are the important cells in the pulmonary epithelial barrier and excessive apoptosis of AECs has been considered as a key process of ALI[5,6], we assessed the effect of *circHECTD1* on AEC apoptosis. Our results showed that *circHECTD1* was also downregulated in LPS-induced human and mouse AECs, and its overexpression repressed the LPS-induced apoptosis of human and mouse AECs. Our further in vivo experiments revealed that *circHECTD1* was also downregulated in the lung tissues of LPS-induced ALI mice and its overexpression increased the survival rate and reduced the lung injury score of ALI mice. Therefore, the present study is the first to elucidate that *circHECTD1* relieves LPS-induced ALI by inhibiting the apoptosis of AECs. Apart from *circHECTD1*, there are many other dysregulated circRNAs in ALI and their roles in ALI need to be further clarified.

Compelling evidence demonstrated that acting as miRNA sponges is a common function of circRNAs. For instance, *circRNA 0060428* contributes to the proliferation of osteosarcoma cells by sponging *miR-375*[29], and *circRNA-CIDN* ameliorates the compression loading-induced injury of nucleus pulposus cells by sponging *miR-34a-5p*[30]. As a member of circRNAs, *circHECTD1* has also been reported to exert its function by sponging miRNAs. In GC, *circHECTD1* can act as a sponge of *miR-1256* to promote glutaminolysis, proliferation, migration, and invasion of GC cells[15]. In cerebral ischemic stroke, *circHECTD1* facilitates the activation of astrocytes via binding to *miR-142* and inhibiting its expression[21]. Based on the bioinformatics analysis, we found that there were predicted binding sites of many miRNAs on the *circHECTD1* sequence, including *miR-136*, *miR-142*, *miR-335*, *miR-199*, *miR-519*, *miR-561*, and *miR-320a*, offering the insight that *circHECTD1* may sponge these miRNAs. To verify this, we evaluated the effect of *circHECTD1* on the expressions of these miRNAs in AECs. The results showed that the knockdown of *circHECTD1* significantly increased the expressions *miR-136* and *miR-320a*, while having no significant impact on the other 6 miRNAs, further implying that *circHECTD1* can function in AEC cells as sponges of *miR-320a* and *miR-136*. More importantly, our RNA-FISH assay visually showed that *circHECTD1* is co-localized with *miR-136* and *miR-320* in the cytoplasm of AEC. The luciferase reporter gene and RNA pull-down assays confirmed that *circHECTD1* was bound to *miR-136* and *miR-320a*. To further investigate the mechanism of *circHECTD1*/miRNAs in ALI, we determined the target mRNAs of *miR-320a* and *miR-136* in the further study.

PIK3CA is an important member of the PI3K family, whose amplification constitutively activates the PI3K/Akt signaling pathway[31]. In ALI, activation of the PI3K/AKT signaling pathway can reduce the apoptosis rate of type II AECs through regulating many downstream targets (such as Bad, Bax, and caspase-9), thus protecting lung tissues[32]. Besides, the previous study also showed that the expression of PIK3CA/Akt can mediate the role of *miR-203* in LPS-induced apoptosis of AECs[33]. Similarly, in the present study, we confirmed that *miR-320a* could target PIK3CA and the forced expression of *miR-320a* reduced the expression of PIK3CA in AECs. The overexpression of *circHECTD1* promoted the activation of the PIK3CA/Akt pathway in LPS-induced AECs, while *miR-320a* overexpression reversed this effect. Furthermore, our results showed that the overexpression of *circHECTD1* inhibited LPS-induced apoptosis of AECs, and PIK3CA knockdown abolished this impact. Hence, these results indicated that *circHECTD1* inhibited AECs apoptosis via *miR-320a*/PIK3CA pathway.

Sirt1 is a histone deacetylase dependent on nicotinamide adenine dinucleotide (NAD^+) in the Sirtuins family and is closely associated with anti-apoptosis[34]. Previous studies have confirmed that SIRT1 inhibits the expression of Bax by deacetylating P53, which is a key gene regulating cell proliferation and apoptosis and thus suppressing cardiomyocyte apoptosis[35]. Also, studies reveal that the activation of Sirt1 can inhibit AEC apoptosis in ALI. In N-methyl-d-aspartate-induced ALI, Sirt1 activation stimulated by oleanolic acid represses the apoptosis of mouse AECs[36]. In LPS-induced ALI, Sirt1 expression in AECs was inhibited and its activation induced by resveratrol reduced LPS-induced apoptosis of AECs[37]. In this study, our luciferase reporter gene assay indicated that *miR-136* targeted Sirt1 and its overexpression downregulated the expression of Sirt1 in AECs. *circHECTD1* overexpression up-regulated the expression of Sirt1 in LPS-induced AECs, while this effect was reversed by *miR-136* overexpression. Furthermore, our results showed that the

overexpression of *circHECTD1* inhibited LPS-induced apoptosis of AECs, and Sirt1 silence abrogated this effect. Hence, these results indicated that *circHECTD1* inhibited AECs apoptosis via the *miR-136*/Sirt1 pathway.

Although our study has achieved some interesting and meaningful findings, it has limitations. As reported, AEC apoptosis can induce damage to the alveolar epithelial barrier, which is composed of AECs and the pulmonary vascular endothelium[5,6]. However, we only studied the role of *circHECTD1* in AEC apoptosis and did not explore the function of *circHECTD1* in the injury of pulmonary vascular endothelium. This will be the subject of our further study. In the future, we will study the influence mechanism of pulmonary vascular endothelium and AECs on the pathogenesis and prognosis of ALI/ARDS, thus providing theoretical basis for the prevention and treatment of ALI/ARDS.

In conclusion, the results of the current study demonstrate that *circHECTD1* attenuates the apoptosis of AECs in LPS-induced ALI through *miR-320a*/PIK3CA and *miR-136*/Sirt1 pathways. This finding may provide a novel therapeutic target for ALI.

DATA AVAILABILITY

All the data generated or analyzed during this study are included in the manuscript.

REFERENCES

1. Villar, J. et al. The ALIEN study: Incidence and outcome of acute respiratory distress syndrome in the era of lung protective ventilation. *Intensive Care Med.* **37**, 1932–1941 (2011).
2. Blank, R. & Napolitano, L. M. Epidemiology of ARDS and ALI. *Crit. Care Clin.* **27**, 439–458 (2011).
3. Bocharov, A. V. et al. Synthetic amphipathic helical peptides targeting CD36 attenuate lipopolysaccharide-induced inflammation and acute lung injury. *J. Immunol.* **197**, 611–619 (2016).
4. Bardales, R. H., Xie, S. S., Schaefer, R. F. & Hsu, S. M. Apoptosis is a major pathway responsible for the resolution of type II pneumocytes in acute lung injury. *Am. J. Pathol.* **149**, 845–852 (1996).
5. MacRedmond, R., Singhera, G. K. & Dorscheid, D. R. Erythropoietin inhibits respiratory epithelial cell apoptosis in a model of acute lung injury. *Eur. Respir. J.* **33**, 1403–1414 (2009).
6. Bem, R. A., Bos, A. P., Matute-Bello, G., van Tuyl, M. & van Woensel, J. B. M. Lung epithelial cell apoptosis during acute lung injury in infancy. *Pediatr. Crit. Care Med.* **8**, 132–137 (2007).
7. Hansen, T. B. et al. Natural RNA circles function as efficient microRNA sponges. *Nature* **495**, 384–388 (2013).
8. Sang, Y. et al. circRNA_0025202 regulates tamoxifen sensitivity and tumor progression via regulating the miR-182-5p/FOXO3a axis in breast cancer. *Mol Ther.* **27**, 1638–1652 (2019).
9. Li, H. et al. Circular RNA circRNA_000203 aggravates cardiac hypertrophy via suppressing miR26b-5p and miR-140-3p binding to Gata4. *Cardiovasc. Res.* **116**, 1323–1334 (2019).
10. Dong, W. et al. Circular RNA ACVR2A suppresses bladder cancer cells proliferation and metastasis through miR-626/EYA4 axis. *Mol. Cancer* **18**, 95–95 (2019).
11. Garikipati, V. N. S. et al. Circular RNA CircFndc3b modulates cardiac repair after myocardial infarction via FUS/VEGF-A axis. *Nat. Commun.* **10**, 4317–4317 (2019).
12. Ye, Z. et al. The differential expression of novel circular RNAs in an acute lung injury rat model caused by smoke inhalation. *J. Physiol. Biochem.* **74**, 25–33 (2018).
13. Li, X. et al. Microarray analysis reveals the changes of circular RNA expression and molecular mechanism in acute lung injury mouse model. *J. Cell. Biochem.* **120**, 16658–16667 (2019).
14. Zhou, Z. et al. circRNA mediates silica-induced macrophage activation via HECTD1/ZC3H12A-dependent ubiquitination. *Theranostics* **8**, 575–592 (2018).
15. Cai, J. et al. circHECTD1 facilitates glutaminolysis to promote gastric cancer progression by targeting miR-1256 and activating β-catenin/c-Myc signaling. *Cell Death Dis.* **10**, 576–576 (2019).
16. Peng, X., Jing, P., Chen, J. & Xu, L. The role of circular RNA HECTD1 expression in disease risk, disease severity, inflammation, and recurrence of acute ischemic stroke. *J. Clin. Lab. Anal.* **33**, e22954–e22954 (2019).
17. Li, X., Yang, L. & Chen, L.-L. The biogenesis, functions, and challenges of circular RNAs. *Mol. Cell* **71**, 428–442 (2018).
18. Han, B., Chao, J. & Yao, H. Circular RNA and its mechanisms in disease: From the bench to the clinic. *Pharmacol. Ther.* **187**, 31–44 (2018).
19. Bi, J. et al. Circ-BPTF promotes bladder cancer progression and recurrence through the miR-31-5p/RAB27A axis. *Aging (Albany NY)* **10**, 1964–1976 (2018).
20. Wei, S. et al. The circRNA circPTPRA suppresses epithelial-mesenchymal transitioning and metastasis of NSCLC cells by sponging miR-96-5p. *EBioMedicine* **44**, 182–193 (2019).
21. Han, B. et al. Novel insight into circular RNA HECTD1 in astrocyte activation via autophagy by targeting MIR142-TIPARP: implications for cerebral ischemic stroke. *Autophagy* **14**, 1164–1184 (2018).
22. Xie, W. et al. miR-34b-5p inhibition attenuates lung inflammation and apoptosis in an LPS-induced acute lung injury mouse model by targeting progranulin. *J. Cell. Physiol.* **233**, 6615–6631 (2018).
23. Dunn, K. W., Kamocka, M. M. & McDonald, J. H. A practical guide to evaluating colocalization in biological microscopy. *American J. Physiol. Cell Physiol.* **300**, C723–C742 (2011).
24. Yang, J. et al. Circular RNA hsa_circRNA_0007334 is predicted to promote MMP7 and COL1A1 expression by functioning as a miRNA sponge in pancreatic ductal adenocarcinoma. *J. Oncol.* **2019**, 7630894–7630894 (2019).
25. Shen, S. et al. CircSERPINE2 protects against osteoarthritis by targeting miR-1271 and ETS-related gene. *Ann. Rheum. Dis.* **78**, 826–836 (2019).
26. Wang, X.-B. et al. circRNA_0006393 promotes osteogenesis in glucocorticoid-induced osteoporosis by sponging miR-145-5p and upregulating FOXO1. *Mol. Med. Rep.* **20**, 2851–2858 (2019).
27. Cheng, Y. et al. CircRNA-012091/PPP1R13B-mediated Lung Fibrotic Response in Silicosis via Endoplasmic Reticulum Stress and Autophagy. *Am. J. Respir. Cell Mol. Biol.* **61**, 380–391 (2019).
28. Fang, S. et al. circHECTD1 promotes the silica-induced pulmonary endothelial-mesenchymal transition via HECTD1. *Cell Death Dis.* **9**, 396–396 (2018).
29. Cao, J. & Liu, X.-S. Circular RNA 0060428 sponges miR-375 to promote osteosarcoma cell proliferation by upregulating the expression of RPBJ. *Gene.* **740**, 144520–144520 (2020).
30. Xiang, Q. et al. CircRNA-CIDN mitigated compression loading-induced damage in human nucleus pulposus cells via miR-34a-5p/SIRT1 axis. *EBioMedicine* **53**, 102679–102679 (2020).
31. Janku, F. et al. Assessing PIK3CA and PTEN in early-phase trials with PI3K/AKT/mTOR inhibitors. *Cell Rep.* **6**, 377–387 (2014).
32. Bao, S. et al. Keratinocyte growth factor induces Akt kinase activity and inhibits Fas-mediated apoptosis in A549 lung epithelial cells. *Am. J. Physiol. Lung Cell Mol. Physiol.* **288**, L36–L42 (2005).
33. Ke, X.-F., Fang, J., Wu, X.-N. & Yu, C.-H. MicroRNA-203 accelerates apoptosis in LPS-stimulated alveolar epithelial cells by targeting PIK3CA. *Biochem. Biophys. Res. Commun.* **450**, 1297–1303 (2014).
34. Zhou, L. et al. Overexpression of SIRT1 prevents hypoxia-induced apoptosis in osteoblast cells. *Mol. Med. Rep.* **16**, 2969–2975 (2017).
35. Mu, W. et al. Overexpression of a dominant-negative mutant of SIRT1 in mouse heart causes cardiomyocyte apoptosis and early-onset heart failure. *Sci. China Life Sci.* **57**, 915–924 (2014).
36. Peng, X.-P., Li, X.-H., Li, Y., Huang, X.-T. & Luo, Z.-Q. The protective effect of oleanolic acid on NMDA-induced MLE-12 cells apoptosis and lung injury in mice by activating SIRT1 and reducing NF-κB acetylation. *Int. Immunopharmacol.* **70**, 520–529 (2019).
37. Liu, X., Shao, K. & Sun, T. SIRT1 regulates the human alveolar epithelial A549 cell apoptosis induced by Pseudomonas aeruginosa lipopolysaccharide. *Cell Physiol. Biochem.* **31**, 92–101 (2013).

AUTHOR CONTRIBUTIONS

L.H.B. and G.M. participated in the experimental design, manuscript writing and manuscript revision. L.H.B., N.X.X., S.H.J., F.M., D.Y.M., S.R.Q., and M.N.L. participated in cell experiments, acquisition of data, data analysis and interpretation. W.H.L. and W.D. participated in animal experiment and histological experiment. All authors read, revised, and approved the final manuscript.

FUNDING

This study was supported by the finding of the Key scientific research projects of henan provincial colleges and universities (NO. 19A320009).

COMPETING INTERESTS

The authors declare no competing interests.

ETHICS APPROVAL

The animal experiments were performed in the Laboratory Animal Center of Zhengzhou University and approved by the Animal Ethics Committee of the First Affiliated Hospital of Zhengzhou University.

ADDITIONAL INFORMATION

Supplementary information The online version contains supplementary material available at https://doi.org/10.1038/s41374-022-00781-z.

Correspondence and requests for materials should be addressed to Hongbin Li or Min Gao.